Journal of the National Academy of Forensic Engineers®

http://www.nafe.org
ISSN: 2379-3252
DOI: 10.51501/jotnafe.v42i1

Vol. 42 No. 1 June 2025

Using Ground Penetrating Radar Techniques in Forensic Structural Engineering

By Chakradhar Gondi, PE (NAFE #1329A), J. Vincent Barnes III, PE, and Michael J. Wightman

Abstract

One of the most powerful non-destructive testing methods in forensic structural engineering is ground penetrating radar (GPR). It is utilized to detect subsurface features such as rebar, voids, and corrosion in concrete. It is also helpful in investigating differential settlements in structures by identifying voids and anomalies in sub-surface soils that can cause structural instability. GPR works by emitting electromagnetic waves that reflect off materials with varying electrical properties, producing 2-dimensional images or profiles of the subsurface. This paper explores the application of GPR techniques in gathering important structural data and identifying subsurface anomalies and defects. Additionally, it also presents case studies from real-world forensic engineering investigations that demonstrate the use of GPR to diagnose structural defects and prepare repair solutions while minimizing project costs. The challenges and limitations of GPR are also discussed. In summary, GPR is an invaluable tool engineers can use to assess the structural integrity and design without damaging the structure.

Keywords

Ground penetrating radar, GPR, non-destructive testing, NDT, structural damage, reinforced concrete, soils, forensic structural engineering

Introduction

In forensic structural engineering, accurately diagnosing structural issues without damaging the structure is an important initial step of investigation. Non-destructive testing (NDT) methods allow engineers to assess a structure's internal condition, construction, and placement of reinforcement. This information can be obtained non-intrusively, thus avoiding any partial demolitions that can further damage the structure and increase costs associated with the examination. Among these NDT methods to evaluate non-visible components, ground penetrating radar (GPR) has gained prominence for its ability to detect subsurface features and anomalies, providing crucial data on structural performance.

GPR is particularly useful in concrete investigations. It is able to detect internal features such as rebar placement configuration, internal and/or underlying voids, reductions in underlying soil support, and rebar corrosion[1]. These findings can determine structural integrity when used to predict the inherent strength and overall conditions of existing material and support conditions. This paper explores the applications of GPR in forensic engineering, highlighting real-world cases where it has been instrumental in detecting structural findings and guiding repair strategies. GPR's technical principles, practical applications, and inherent limitations are discussed to provide a comprehensive understanding of this powerful NDT tool.

The use of GPR in forensic structural engineering is guided by several well-established standards that ensure consistency and reliability in data collection and interpretation. ASTM D6432-19 is the primary guide for surface GPR methods[1]. It describes how to calibrate equipment, collect signals, and interpret subsurface data. ASTM D6087-22 provides a specific method for evaluating asphalt-covered concrete bridge decks using GPR[2]. This is especially useful for detecting delamination or deterioration beneath the asphalt overlay.

The results from GPR methods are often validated by other testing methods. For example, ASTM C1383-23 provides a standard method for measuring the thickness of concrete members using impact echo testing[3]. This is another NDT method often used to complement GPR findings and confirm concrete member dimensions. For corrosion assessment, ASTM C876-22 defines the standard method for measuring corrosion potentials of uncoated

Chakradhar Gondi, PE, 5755 Rio Vista Dr., Clearwater, FL 33760, (727) 610-5524, chakradhargondi@gmail.com

reinforcing steel in concrete[4]. This method is often used alongside GPR to help predict the extent of corrosion in the reinforcing.

Ground Penetrating Radar (GPR): Technical Background

GPR operates by transmitting electromagnetic waves into a material that reflect back when encountering objects or interfaces with contrasting dielectric properties[5]. These dielectric properties are primarily controlled by electrical conductance, material density, and moisture content. GPR consists of a set of integrated electronic components that transmits high-frequency electromagnetic waves and records the energy reflected back to the material surface. The typical frequency range used for forensic studies ranges from 800 megahertz (MHz) to 2.6 gigahertz (GHz). The GPR system consists of an antenna, which serves as both a transmitter/receiver and a profiling recorder that both processes the incoming signal and provides a graphic digital display of the data. The GPR data can be reviewed and analyzed in real time or recorded for later review using specialized analysis software.

A GPR survey provides a graphic cross-sectional view of subsurface conditions. This cross-sectional view is created from the reflections of repetitive short-duration electromagnetic (EM) waves that are generated as the antenna is moved across the surface. The reflections occur at the subsurface boundary contacts between materials with differing electrical properties. The GPR method is commonly used to identify such targets as thickness of concrete, configuration and placement of rebar, internal or external voids, underground utilities, underground storage tanks or drums, buried debris, or geological features.

A GPR survey is conducted along survey lines (transects), which are measured paths along which the GPR antenna is moved. Horizontal and vertical scale are integrated into the GPR graphic output along with an electronic marker to indicate the current antenna position. This electronic marker and scales allow for a correlation between the GPR data and the position of the GPR antenna on the surface along with an estimated depth of any target of interest.

The greater the electrical contrast between the surrounding materials (earth or concrete) and target of interest, the greater the amplitude of the reflected return signal. Unless the buried object is metal, only part of the signal energy will be reflected back to the antenna. The remaining portion of the signal continues to propagate downward to be reflected by deeper features. When the GPR signal encounters metal, the high electrical conductivity and permittivity of the material cause all of the signal energy to be reflected back to the antenna, resulting in a strong, high-amplitude response that is easily identifiable in the GPR data.

It is noted that because of the 100% reflection that it is not possible to identify any objects that are directly below the metallic object. However, if there is little or no electrical contrast between the target and surrounding earth materials, it will be very difficult (if not impossible) to identify the object using GPR. For example, steel rebar surrounded by concrete is very easily detected, but a PVC conduit that is filled with water that is below the water table may be very difficult to detect. This is because both the PVC water pipe and the surrounding saturated soils would have similar dielectric properties, resulting in low electrical contrast and a very weak or non-existent signal reflection. In contrast, steel rebar in concrete creates strong reflections due to the distinct contrast in dielectric properties between concrete and rebar.

The depth of penetration of the GPR signal is also reduced as the antenna frequency is increased. However, as antenna frequency is increased, the resolution of the GPR data is improved. Therefore, when designing a GPR survey, a tradeoff is made between the required depth of penetration and desired resolution of the data. As a rule, the highest frequency antenna that will still provide the desired maximum depth of penetration should be used.

For many void studies focused on detecting voids in soils beneath structures, an antenna frequency of 800 to 900 MHz is often used. Most rebar and concrete characterization studies are completed using antennas with a frequency of above 1.5 GHz. Depending on the objectives of an investigation, multiple frequency antennas may need to be used for the same project area. For example, a void study might also require that the thickness of the concrete slab and design of the reinforcement be determined.

It should be noted that the penetration depth of the GPR signal can be greatly impacted by the age of the concrete. While newly poured concrete is going through the initial curing process, the signal penetration depth will be significantly reduced due to the elevated conductivity of the concrete that is caused by the high moisture content. It is the author's experience that a minimum of two weeks be allowed before attempting a GPR study for a concrete structure.

Application of GPR in Concrete Rebar Mapping and Corrosion Evaluation

In structural investigations, verifying rebar placement configuration and in-place condition is essential to ensure compliance with design specifications and assess structural safety. GPR can accurately map rebar depth and configuration, identify missing reinforcements, and evaluate corrosion[6].

GPR can be integrated with other complementary NDT tools to extend its capabilities and also help confirm the GPR results[7]. Some of these complementary NDT tools include impact echo (IE), electromagnetic (EM) meters, and half-cell corrosion potential testing.

The IE method is used for thickness evaluations and to assess the condition of concrete slabs, walls, and beams[8]. The method requires access to only one surface of the target area. The concrete thickness accuracy of the IE method is +/- 2% when it is possible to calibrate the instrument to a known concrete thickness at the site. The IE equipment consists of a portable hand-held unit with an electro-mechanical solenoid that generates acoustic compressional waves that reflect back from the bottom or back of the tested member or from a discontinuity or debonding surface within the concrete. The response of the IE system is then measured by the acoustic receiver mounted next to the solenoid impact point and analyzed. The instrument produces a real-time waveform display while testing. For each data point collected, multiple waveform "stacks" are recorded and used to produce the final estimated thickness. The data can also be recorded for further analysis.

EM devices consist of a set of integrated electronic components that can detect the presence of metallic objects within concrete. The system operates on the principle of pulse induction where a primary EM field is created by the equipment. Any metallic objects within the equipment's sensitivity range will have created within them a secondary EM field that is sensed by the equipment. Modern EM devices can also provide an estimate of cover depth and rebar size for simple rebar configurations and where the bars are sufficiently spaced far enough apart.

It should be noted that while GPR is effective for locating reinforcement in concrete and estimating cover depth, it is not typically reliable for accurately determining rebar diameter — particularly for smaller bar sizes[9]. Although GPR can detect rebar and provide an approximate indication of bar size based on using advanced processing techniques, more precise estimation often requires complementary tools, such as EM devices. In most studies, the estimated rebar diameter is reported as plus/minus one bar size. The rebar survey results obtained from GPR and EM systems are best validated through destructive testing methods such as coring, which provide direct physical confirmation of the reinforcement size.

The half-cell potential method is used to monitor the corrosion of steel rebar in concrete. Half-cell testing is performed by connecting one electrode (the base electrode) to an exposed piece of rebar within the concrete and placing a second electrode (roving electrode) at testing locations across the concrete surface. The potential response between the two electrodes is measured in millivolts (mV). This test may involve selective chipping of concrete at test locations to expose the rebar. Using the rebar layout from GPR data, half-cell tests can focus on specific regions where moisture or concrete anomalies are detected, allowing for a more targeted and efficient corrosion assessment[10]. Based on the ASTM C876-09 standards, half-cell measurements of less than -350 mV are considered to indicate with a greater than 90% probability of rebar corrosion. Values between -200 to -349 mV are considered to indicate uncertain conditions, and values greater than -200 mV and above are considered to have less than 10% probability of rebar corrosion[4].

Figure 1 and **Figure 2** show GPR data samples from a geophysical investigation performed by the authors for a warehouse metal frame building in Clearwater, Florida. This geophysical investigation was performed at multiple locations throughout the concrete first floor slab, exterior wall foundations, and interior column foundations of the building. The existing building foundations were required to be analyzed for increase in loading due to new proposed additions on the roof. Since original as-built drawings of the building were not available, a GPR survey was performed to document foundation size and location of steel

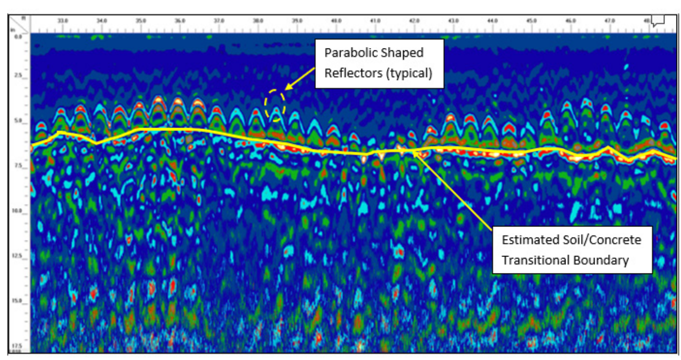

Figure 1
GPR data sample at concrete slab.

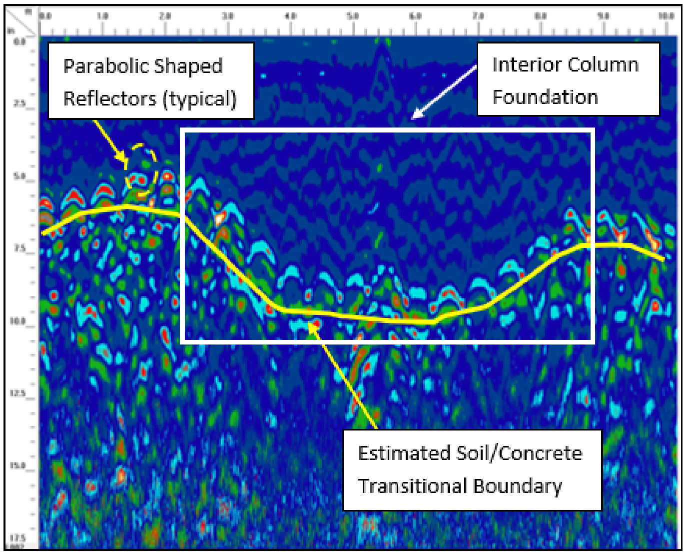

Figure 2
GPR data sample at interior column foundation.

reinforcement. To validate the results, the GPR survey was supplemented with additional NDT methods, including EM and IE techniques. The IE testing was conducted in accordance with ASTM C1383 to determine the thickness of concrete elements. The EM survey was performed using the Proceq 650 AI, which is capable of identifying rebar to a maximum depth of 5 to 7 inches. The features observed on GPR data that are most commonly associated with rebar are:

- The occurrence of high-amplitude parabolic-shaped GPR reflectors.
- If the reinforcing is continuous, the associated GPR reflectors should match in both estimated depth below surface and lateral position on parallel GPR transect lines.

The horizontal scale in the sample two-dimensional GPR scans shown in **Figure 1** and **Figure 2** represents longitudinal distance in feet, while the vertical scale denotes the depth within the concrete member in inches. The peaks of the hyperbola in **Figure 1** and **Figure 2** clearly define the position of the rebars, while the distance between the peaks represents the spacing between each rebar[6].

Based on the scan data, a single layer of reinforcement was identified near the bottom of the slab. Reinforcement was present in both orthogonal directions; one direction is visible in the figures, and the perpendicular direction was confirmed from a separate set of GPR transects performed orthogonal to those shown and correlated with typical construction practices. The GPR data also identified the transition boundary between the concrete and supporting soil, allowing for the thickness of the concrete slab to be estimated.

The GPR investigation determined that the concrete slab for the main building ranges in thickness from 5.5 to 6.5 inches (**Figure 1**) and is reinforced with a rebar mat on 6-inch spacing. Using EM, the rebar size is estimated to be either #4 or #5 , with a cover depth ranging from approximately 4.5 to 5.5 inches (**Figure 1**). The interior column foundation does not appear to be a separate pad, but rather an excavated thickening of the floor slab (**Figure 2**). The foundation width at the bottom is approximately 3-foot by 3-foot, and the maximum thickness at center of foundation is approximately 10 to 12 inches. No additional reinforcement — besides what is present in overall slab — is observed within the foundations.

Application of GPR in Identifying Possible Voids

Voids in soils beneath a structure can lead to differential settlement and instability of foundations and floor slab systems. GPR assists in detecting such voids, particularly in areas where soil erosion, poor compaction, or subsurface water flow have occurred. Identifying these voids helps engineers devise solutions to stabilize foundations, protecting against future settlement and structural damage. The features observed on GPR data that are most commonly associated with void formation are:

- A downwarping of GPR reflector sets that is associated with suspected lithological contacts toward a common center. Such features typically have a bowl or funnel-shaped configuration and can be associated with a deflection of overlying sediment horizons caused by the migration of sediments into underlying voids. If the GPR reflector sets are sharply downwarping and intersect, they can create a “bow-tie”-shaped GPR reflection feature, which often designates the apparent center of the GPR anomaly.
- A localized significant increase in the depth of the penetration and/or amplitude of the GPR signal response. The increase in GPR signal penetration depth or amplitude is often associated with void formation.
- An increase in the amplitude of horizontal reflector sets below the concrete slab indicating an air space void.

The case study in the next section is a real-life project example that demonstrates how GPR was used effectively to identify anomalies in subsurface soils to prepare solutions for a loading dock slab repair.

Case Study — Loading Dock Slab Settlement Investigation

A loading dock slab for an office facility located in Tampa, Florida began exhibiting signs of settlement, including noticeable cracks and uneven surfaces that disrupted operations (**Figures 3, 4,** and **5**). The building served by the loading dock is a seven-story office building built approximately in 2007. The loading dock area consists of an elevated concrete slab that rises about 4 ft from the ground surface and a concrete retaining stem wall. This area is being used for loading/unloading the shipping supplies of various businesses in the building. The slab and retaining wall itself are independent structures and not connected to the main building. The slab is tied into the retaining wall with rebar dowels.

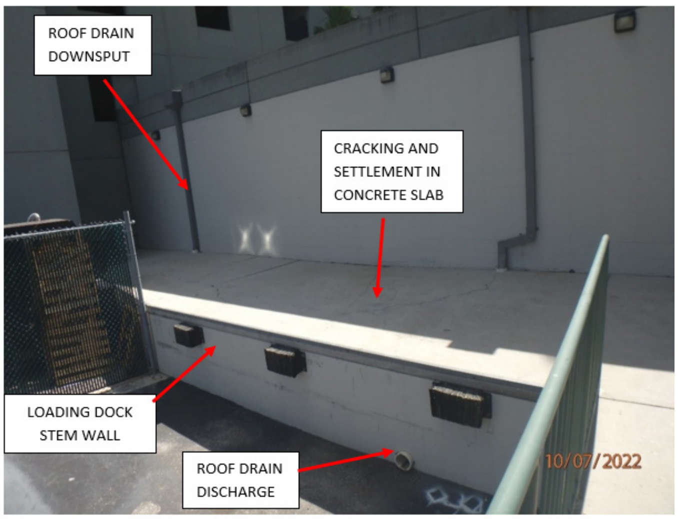

Figure 3
Loading dock area.

Figure 4
Up to ½-inch-wide crack across the slab.

A forensic investigation using GPR survey was performed across the loading dock area to identify and locate any possible voids or heterogeneities (e.g., buried debris) in the soil underneath the concrete slab that could be associated with the differential settlement and concrete cracking. The GPR survey was conducted along a grid series of GPR transects that were spaced 2 ft apart, as shown in **Figure 6**. The GPR data was collected using two GPR systems.

A high-resolution imaging of soil conditions directly below the slab was obtained using GSSI Mini Structure Scan with a 2.6 GHz antenna with a time range setting of 10 nanoseconds. This provided a very high-resolution imaging of soil conditions directly below the slab to a depth of approximately 1.5 ft below land surface (bls). The

Figure 5
Up to 2 inches of slab drop in the eastern edge.

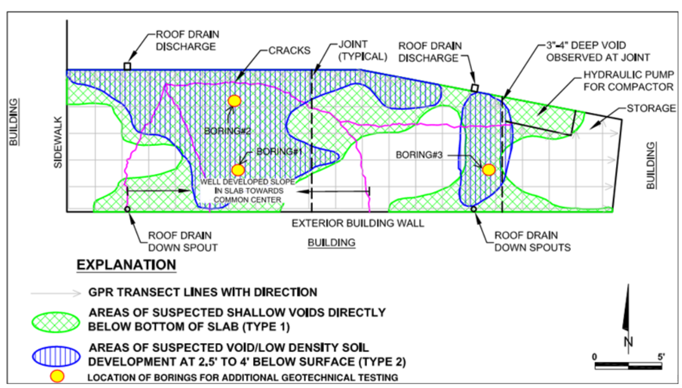

Figure 6
Site map showing results of GPR investigation.

assessment of deeper soil conditions was completed using a GSSI SIR 3000 with a 900 MHz antenna and a time range setting of 30 nanoseconds. This equipment configuration provided an estimated depth of investigation of 2 to 3 ft bls.

The results of the geophysical investigation are presented in **Figures 6, 7,** and **8**. Based on the GPR results, the authors identified two types of anomalous subsurface conditions. Type 1 anomalies are suspected shallow voids directly below the bottom of the slab. For the majority of the anomaly areas, these voids appear to be less than 0.25 inches in height. However, in some areas, they could be up to 3 to 4 inches in height — as was observed at the northern end of the slab joint in the eastern portion of the site. Type 2 anomalies are characterized by a localized increase in the amplitude of the GPR signal response at a depth range of 2.5 to 4 ft bls. Examples of the GPR data collected across each of the Type 1 and Type 2 anomaly areas are provided in **Figure 7** and **Figure 8**. The coloration of the interpreted voids in **Figures 7** and **8** was produced by the equipment software, which offers options for selecting

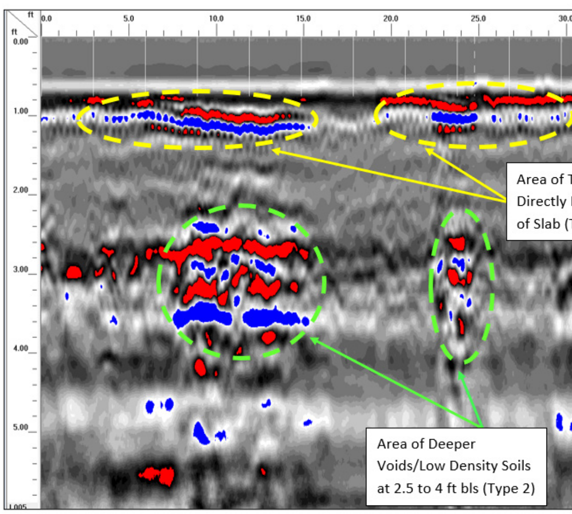

Figure 7
GPR data collected with 900 Mhz antenna.

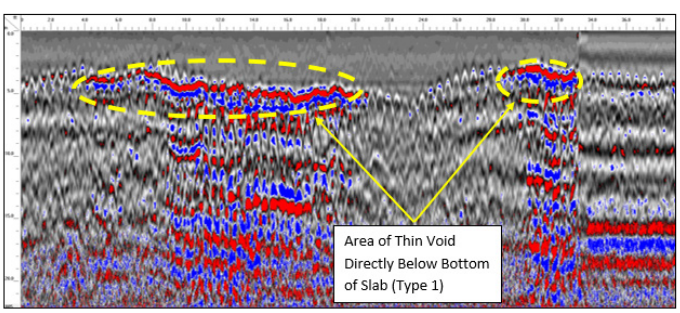

Figure 8
GPR data collected with 2.6 GHz antenna.

both the color palette and how the amplitudes of the returns are displayed. Further evaluation of these GPR study results indicated the following:

- Type 1 and Type 2 anomalies are present in the majority of the area where the concrete slab is sloping to a common center in the western portion of the slab.

- Type 1 and Type 2 anomalies are present along the entire route of the eastern roof drain but are only present in a portion of the western roof drain.

- Type 2 (deep) anomalies are present within the entire lateral extent of the Type 1 (shallow) anomalies.

- The original building structural drawings indicated that the slab construction is 5 inches thick with 6x6-W2.9xW2.9 welded wire reinforcement (WWR). The GPR results, as shown in **Figure 8**, determined that the concrete slab thickness ranged from approximately 2.5 to 5 inches, based on the depth of the last consistent horizontal reflector before signal attenuation. The regular spacing and consistent pattern of low-amplitude hyperbolic reflections observed near the bottom of the slab suggested a rebar or mesh pattern with a 6-inch grid spacing. However, as previously discussed, GPR has limitations in distinguishing fine mesh elements from closely spaced small-diameter rebar, particularly when the wire is of a smaller gauge.

It was considered that the GPR anomalies were associated with voids or low-density soils/buried debris. Hence, a follow-up shallow geotechnical soil testing was performed in this area to evaluate the soil profile and confirm the GPR findings of any suspected voids. A total of three hand auger borings were drilled into existing concrete slab and soil fill to a depth of about 5 ft below top of slab or auger refusal. A dynamic cone penetrometer (DCP) test was performed at each hand auger location to evaluate soil density in the upper approximate 4 to 5 ft of the soil profile[11]. The soil samples were also visually classified soil samples in the laboratory using the Unified Soil Classification System[12].

The results of soil profiles from hand auger borings is shown in **Figure 9**. The summary of lime rock bearing ratio (LBR) results obtained from DCP tests at each hand auger location is presented in **Figure 10**. The LBR is

Depth (feet) From	To	Material Description
HA-01		
0	0.5	2 inches of void below 4 inches thick slab core
0.5	1.5	Gray fine sand (SP) with rock fragments and clay clods
1.5	2.5	Gray fine sand (SP) with rock fragments, plastic sheet, burnt wood, and clay clods
2.5	3.5	Gray fine sand (SP) with roots and metal debris
3.5	5.0	Gray fine sand (SP) with rock fragments and clay clods
HA-02		
0	0.75	4.75 inches of void below 4.25 inches thick slab core
0.75	2.5	Gray fine sand (SP) with clay clods
2.5	4.5	Gray fine sand with fragments of old cast iron pipe
HA-03		
0	0.5	3 inches of void below 3 inches thick slab core
0.5	4.5	Gray fine sand (SP) with clay clods and limerock fragments
4.5	5.0	Gray fine sand (SP) with fragments of shells and limerock

Figure 9
Summary of hand auger boring results.

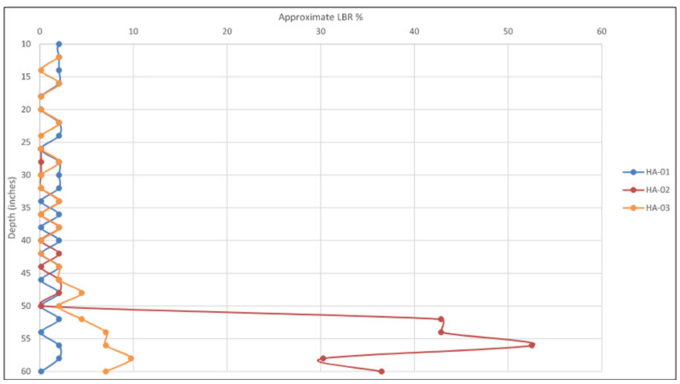

Figure 10
Relative subgrades density vs depth at hand auger boring results.

a measure of soil strength commonly used in Florida for evaluating roadway subgrades. It is a variation of the California Bearing Ratio (CBR), which is used outside of Florida with the conversion LBR = 1.25 × CBR[13]. The DCP test was conducted in accordance with ASTM D6951, where the number of blows over a specific depth interval was converted to an equivalent CBR or LBR percentage.

Essentially, LBR quantifies the relative strength of a material as a percentage of lime rock strength, with higher values representing greater compaction and lower values indicating looser material. Different materials have characteristic maximum LBR values when properly compacted. For instance, crushed concrete typically has an LBR of around 150%. Lime rock (limestone) has a standard LBR of 100%, meaning an LBR of 100% represents material strength equivalent to that of lime rock. Clean fine sand, when well-compacted, typically has an LBR of 20% to 22%[14].

Further evaluation of the geotechnical testing results from **Figures 9** and **10** indicated:

- Hand auger borings and DCP soundings indicated that the supporting soil is very loose and filled with buried debris, which confirmed the Type 2 (deep) anomalies depicted in the GPR survey results shown in **Figures 6** through **8**.

- In **Figure 10**, all recorded LBR values were below 5%, indicating that the soil beneath the loading dock slab is extremely loose. If the soil had been properly compacted or had not experienced degradation due to material loss, the LBR should have been at least 15 to 20%[14]. Additionally, the DCP data for hand auger #3 showed a few outliers corresponding to higher LBR percentages at greater depths, which likely indicate obstructions or very hard materials within the soil profile.

- These results indicated that the soil underneath the loading dock slab contained debris (burnt wood, debris and other unsuitable material) prior to filling the area for the construction of the dock. Debris inherently contained void spaces, and, over time, soil gradually migrated into these openings. This soil migration loosened the soil and caused settlement, which resulted in the settlement of the slab itself.

- Since the loading dock was constructed as a soil-supported slab, the supporting soil settlement led to distress in the concrete slab through differential settlement and concrete cracking.

Based on the results of the GPR survey and geotechnical soil testing, recommendations were provided for the complete removal of all existing loading dock slab and the underlying fill soil to a depth of at least 4 ft below the top of the slab. Subsequently, the forensic team designed a new replacement slab and new compacted fill under the slab in loading dock area. The new slab was tied into the existing 4-ft-tall concrete stemwall with rebar dowels. Additionally, existing roof drain downspout pipes, which pass under the loading dock slab and discharge at the bottom of the concrete stem wall, were examined during the excavation and removal of the existing slab and soil fill. The existing roof drain pipes were found to be intact, free from debris, and without leaks. As a result, the existing drain pipes were salvaged and reused with the new slab and soil fill.

Challenges and Limitations of GPR in Structural Investigations

While GPR is a valuable tool in forensic investigations, it does have limitations that engineers must consider. The analysis and collection of GPR data is both a technical and interpretative skill. Misinterpretation of the findings can lead to unnecessary repairs or overlooked issues. The technical aspects of GPR investigations are learned from both training and experience. Having the opportunity to compare GPR data collected in numerous settings to the results from geotechnical and structural studies performed at the same locations allows the forensic engineer to develop interpretative skills for soil and concrete characterization studies.

The penetration depth of GPR is limited by the frequency of the electromagnetic waves and the material's properties. For instance, highly conductive materials (like wet clay or metal-reinforced concrete) can significantly reduce depth penetration. Selecting the appropriate frequency is critical but often involves trade-offs between resolution and depth.

The ability of GPR to collect interpretable information at a project site is limited by the attenuation (absorption) of the GPR signal by underlying soils. Once the GPR signal has been attenuated at a particular depth, information regarding deeper geological conditions will not be obtained. GPR data can only resolve subsurface features that have a sufficient electrical contrast between the feature in question and surrounding earth materials. If an insufficient contrast is present, the subsurface feature will not be identified.

Environmental factors, such as moisture, metal inclusions, and closely spaced rebar, can interfere with GPR signals, creating noise that complicates data interpretation. Thus, the forensic engineer should consider complementary NDT or destructive methods necessary to confirm findings or improve accuracy.

Conclusion

GPR has proven to be an indispensable tool in forensic structural engineering, offering non-destructive insights into subsurface conditions that are critical for structural assessment. Through case studies, this paper has demonstrated GPR's application in rebar mapping, void detection, and corrosion assessment, highlighting its cost-effectiveness and diagnostic precision. While GPR has limitations, such as depth restrictions and sensitivity to environmental conditions, its advantages make it a valuable resource for engineers seeking to preserve structural integrity without invasive testing. Pairing the GPR technology with other complementary NDT tools like impact echo, electromagnetics, and half-cell potential tests — or with limited destructive testing or borings — will further enhance its applications and accuracy in forensic investigations.

References

1. ASTM D6432-19: Standard Guide for Using the Surface Ground Penetrating Radar Method for Subsurface Investigation, ASTM International, West Conshohocken, PA, USA, 2019.

2. ASTM D6087-22, “Standard Test Method for Evaluating Asphalt-Covered Concrete Bridge Decks Using Ground Penetrating Radar,” ASTM International, West Conshohocken, PA, USA., 2022.

3. ASTM C1383-23, “Standard Test Method for Measuring the P-Wave Speed and the Thickness of Concrete Plates Using the Impact-Echo Method,” ASTM International, West Conshohocken, PA, USA, 2023.

4. ASTM C876-22b, “Standard Test Method for Corrosion Potentials of Uncoated Reinforcing Steel in Concrete,” ASTM International, West Conshohocken, PA, USA, 2022.

5. A. P. Annan, Ground Penetrating Radar: Principles, Procedures, and Applications, 1st ed, Ontario: Sensors & Software Inc., 2003.

6. K. Tešić, A. Baričević and M. Serdar, “Comparison of cover meter and ground penetrating radar performance in structural health assessment: case studies,” Građevinar (Zagreb), vol. 73 (11), pp. 1131-1144, 2021-12.

7. A. Elseicy, A. Alonso-Díaz, M. Solla, M. Rasol and S. Santos-Assunçao, “Combined Use of GPR and Other NDTs for Road Pavement,” Remote sensing (Basel, Switzerland), vol. 14 (17), p. 4336, 2022.

8. M. Sansalone, J. LIN and W. B. STREETT, “Determining Concrete Highway Pavement Thickness Using Wave Speed Measurements and the Impact-Echo Method,” Structural Materials Technology, pp. 348-353, 1996.

9. W. Cheng, H.-H. Sun, K. H. Tan, and Z. Fan, "Estimating the diameter of reinforcing bars using an ultra-wideband MIMO GPR array," Construction and Building Materials, vol. 365, p. 129924, 2023-02.

10. FPRIME C SOLUTIONS, "How to use GPR in Structural Assessment?," 7 OCTOBER 2020. [Online]. Available: https://fprimec.com/how-to-use-gpr-in-structural-assessment/.

11. ASTM D6951/D6951M-18, "Standard Test Method for Use of the Dynamic Cone Penetrometer in Shallow Pavement Applications," ASTM International, West Conshohocken, PA, 2018.

12. ASTM D2487-17, Standard Practice for Classification of Soils for Engineering Purposes (Unified Soil Classification System), West Conshohocken, PA: ASTM International,, 2017.

13. W. VIRGIL PING, LING GE, AND ZHILIANG YU, "Evaluation of Pavement Bearing Characteristics Using Florida Limerock Bearing Ratio Test," TRANSPORTATION RESEARCH RECORD, vol. 1547, no. 1, pp. 53-60, 1996.

14. Iowa Department of Transportation, Iowa State University, "Iowa Statewide Urban Design and Specifications (SUDAS), Section 6E-1 – Subgrade Design and Construction," 2013. [Online]. Available: https://www.intrans.iastate.edu/wp-content/uploads/sites/15/2020/03/6E-1.pdf. [Accessed 29 5 2025].